Synthesis and Structural Characterization of Potassium Salts of Phosphane-Substituted (Cyclopentadienyl)iron Dicyanides, and Their Use as Bridging Ligands for Copper(I) Phosphane Derivatives

Donald J. Darensbourg,*[a] M. Jason Adams,[a] Jason C. Yarbrough,[a] and Andrea L. Phelps[a]

Dedicated to the memory of Professor Dieter Sellmann, a good friend and brilliant chemist

Keywords: Cyanides / Heterometallic complexes / Bridging ligands / Iron / Copper / Potassium

Phosphane-substituted $CpFe(CN)_2$ anions have been synthesized by photochemical decarbonylation of $KCpFe(CN)_2CO$ in the presence of various mono- and diphosphanes. The synthesis and characterization of uniquely bridged diphosphane derivatives, $[KCpFe(CN)_2]_2$-μ-$(Ph_2P)_2$–$(CH_2)_n$ (n = 2–4), are particularly noteworthy. These phosphane-substituted $CpFe(CN)_2^-$ units have afforded stable mixed-metal complexes upon reaction with Cu^I in the presence of tricyclohexylphosphane in acetonitrile solution. X-ray crystallography shows these derivatives to display two-dimensional diamond-shaped structures with copper(I) of the form $[Fe(CN)_2Cu]_2$, where the Cu^I centers exhibit both trigonal and tetrahedral geometries. Infrared data reveal that the withdrawal of electron density from the iron centers in these mixed metal cyanides via the cyanide ligands is enhanced upon replacing CO in $CpFe(CN)_2CO^-$ with phosphanes.

Introduction

The use of substitutionally inert organometallic cyanides as ligands to other metal ions has received much interest due to their ability to simplify studies utilizing cyanide as a bridging group.[1] Although, metal hexacyanide salts have long been known to complex other metal ions through bridging cyanide ligands, the resulting derivatives are often highly insoluble aggregates which are difficult to definitively characterize.[2] Organometallic derivatives having the three facial coordination sites occupied by an ancillary ligand, e.g., the cyclopentadienyl moiety, have been used to limit the degree of aggregation.[3] Substitution of the metal center by an additional strongly bonded ligand, such as a tertiary phosphane, further limits bridging in a multidimensional fashion. In addition to promoting solubility, phosphane adducts of these organometallic cyanides provide a convenient ^{31}P NMR probe for studying these complexes. Despite these advantages, relatively few studies have involved these simple metallocyanides.[4]

Vahrenkamp and co-workers have investigated neutral iron monocyanide complexes of the type CpFe(dppe)CN, where dppe = 1,2-bis(diphenylphosphanyl)ethane, as bridging ligands to other metal complexes.[5] The use of metal monocyanide derivatives is particularly beneficial at restricting the bridging capacity of the complex, and thus uncomplicating the study of the cyanide ligand as an electronic linkage between two metal centers. The chelated phosphane ligand serves to block any sites on the iron ion that a more labile ligand might leave open for substitution. Furthermore, the bulkiness of the phosphane ligand often aids in crystallization of the resulting multinuclear metal complexes. Indeed, this simple metallocyanide has allowed Vahrenkamp to examine in detail the redox chemistry of cyanide-bridged trimetallic complexes using cyclic voltammetry. One such study involved the effect of linear vs. bent bridging motifs in the Fe−CN−Pt−NC−Fe metallocyanide unit on electronic communication between the metal centers.[5,6]

A long standing focus in our research efforts involves the design of homogeneous catalysts for the copolymerization of epoxides and carbon dioxide to provide polycarbonates.[7] Relevant to this subject double metal cyanide derivatives, especially those of Fe(II and III) or Co^{III} and Zn^{II}, have received attention as heterogeneous catalysts for this process in the patent literature.[8] In our efforts to synthesize novel mixed-metal cyanides as models for these catalysts, a series of metal complex salts of the general formula $[K][CpFe(CN)_2PR_3]$ have been prepared and characterized both in solution and in the solid state. In addition, the employment of traditionally chelating phosphane ligands have extended the range of these salts to include diiron deriva-

[a] Department of Chemistry, Texas A&M University, College Station, Texas 77843, USA
Fax: (internat.) + 1-979/845-0158
E-mail: djdarens@mail.chem.tamu.edu

tives of the type $[K]_2[CpFe(CN)_2PR_2(CH_2)_nPR_2(CN)_2FeCp]$, where $n = 2-4$ and R = Ph, thereby affording unique bridging ligands with specific bite angles. Importantly, the electronic character of the cyanide ligands can be tailored by choosing phosphanes of the appropriate basicity. Examples of the viability of these anionic metallocyanide derivatives of iron as ligands towards copper(I) are demonstrated with the isolation and crystallographic characterization of the mixed-metal complexes $[CpFe(PPh_3)(\mu\text{-}CN)_2Cu(PCy_3)]_2$ and $Cu(PCy_3)[CpFe(\mu\text{-}CN)_2]_2Cu(PCy_3)_2$-μ-dppp [dppp = 1,2-bis(diphenylphosphanyl)propane].

Results and Discussion

A series of phosphane (= L) substituted salts of $[K][CpFe(CN)_2L]$ has been prepared through photolytic decarbonylation of the parent $[K][CpFe(CN)_2CO]$ compound (Scheme 1). The impetus for these studies comes from our desire to synthesize well-defined double-metal cyanide (DMC) complexes to serve as soluble structural and reactivity models for those employed as heterogeneous catalysts for the polymerization of epoxides to polyols or epoxides and CO_2 to polycarbonates/cyclic carbonates. Relevant to these studies we have previously noted that upon treating analogous DMC complexes derived from the $CpFe(CN)_2CO^-$ anion with excess PCy_3, the reaction according to Equation (1) occurred over an extended reaction time. That is, the metal aggregate was disrupted to afford a trigonal copper(I) center and PCy_3 had displaced CO at the iron center (**A**).[9] Hence, an obvious concern is whether dimer disruption is a necessary structural prerequisite upon substitution of the CO ligand at the iron center with a sterically demanding phosphane ligand.

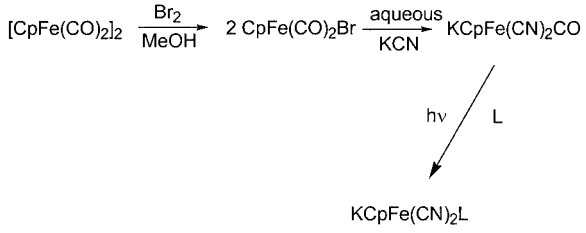

Scheme 1

$$[CpFe(CO)(\mu\text{-}CN)_2Cu(PCy_3)_2]_2 + 2\,PCy_3 \rightarrow 2\,CpFe(PCy_3)(CN)(\mu\text{-}CN)Cu(PCy_3)_2 + 2\,CO \quad (1)$$

In order to tailor the electronic and structural properties of the ancillary metal center we have photochemically substituted the CO ligand in the $KCpFe(CN)_2CO$ salt with various phosphane and diphosphane ligands. A mixture of methanol and acetonitrile was utilized to solubilize both the parent salt and in this instance PPh_3, respectively. Solubility of the reagents, especially the $KCpFe(CN)_2CO$ derivative, is

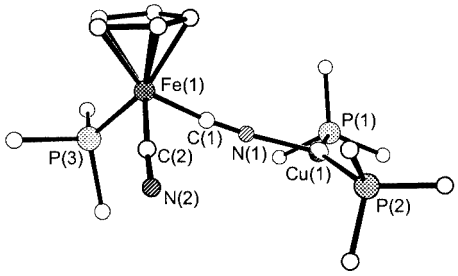

A

essential for complete conversion into product. This complex has alternatively been prepared thermally from $CpFe(CO)(PPh_3)I$ and KCN in refluxing ethanol by Reger.[4] The product, $KCpFe(CN)_2PPh_3$ (**1**), exhibited ν(CN) frequencies at 2055 vs, 2040 s, and 2028 sh cm^{-1} in methanol, which are shifted to lower wavenumbers when compared to the parent compound (see Table 1). This shift to lower frequencies is expected as the result of replacing the carbonyl ligand by primarily a donor phosphane ligand, thereby allowing the cyanide groups to be involved in greater π-backbonding with the iron center. The ^{31}P NMR spectrum of **1** displays a downfield chemical shift from that of the free ligand to δ = 86.9 ppm. The more basic methyldiphenylphosphane ligand was incorporated at the iron center for comparison with the PPh_3 analog, where the only other variance arises from its slightly reduced cone angle of 136 vs. 145° for PPh_3.[10–12] In this instance it was not necessary to employ a mixed-solvent system for the photolytic reaction since both the $KCpFe(CN)_2CO$ salt and PPh_2Me are soluble in methanol. As expected, the increased basicity of the monomethylated phosphane causes the ν(CN) vibrations in $KCpFe(CN)_2PPh_2Me$ (**2**) to shift to lower wavenumbers at 2050, 2034, and 2025 cm^{-1}. The ^{31}P NMR chemical shift in complex **2** appears at δ = 71.3 ppm. Interestingly, in an attempt to improve reaction yields, photolysis of the carbonyl salt with a fourfold excess of PPh_2Me afforded the bis(phosphane) neutral complex $CpFe(CN)(PPh_2Me)_2$ (**3**).

Table 1. Infrared and ^{31}P NMR spectroscopic data (all spectra were determined in methanol solution except for those of compound **3** which were determined in THF)

Compound	ν(CN) [cm^{-1}]	δ [ppm]
$KCpFe(CN)_2(CO)$	2095, 2084	N/A
$KCpFe(CN)_2(PPh_3)$ (**1**)	2055 vs, 2040 s, 2028 sh	86.9
$KCpFe(CN)_2(PPh_2Me)$ (**2**)	2050 vs, 2034 s, 2025 sh	71.3
$CpFe(CN)(PPh_2Me)_2$ (**3**)	2069	57.2
$[KCpFe(CN)_2]_2$ μ-dppe (**4**)	2050, 2032, 2025 sh	78.2
$[KCpFe(CN)_2]_2$ μ-dppp (**5**)	2050, 2032, 2025 sh	77.0
$[KCpFe(CN)_2]_2$ μ-dppb (**6**)	2050 vs, 2034 s, 2026 sh	76.5
$[KCpFe(CN)_2]_2$ μ-dppa (**7**)	2057 s, 2050 vs, 2032 sh	64.9

A number of bidentate phosphanes have been utilized as bridging ligands between two $CpFe(CN)_2$ anionic units. These derivatives were synthesized by photolysis of the parent salt $KCpFe(CN)_2CO$ in the presence of 0.5 equiv. of the

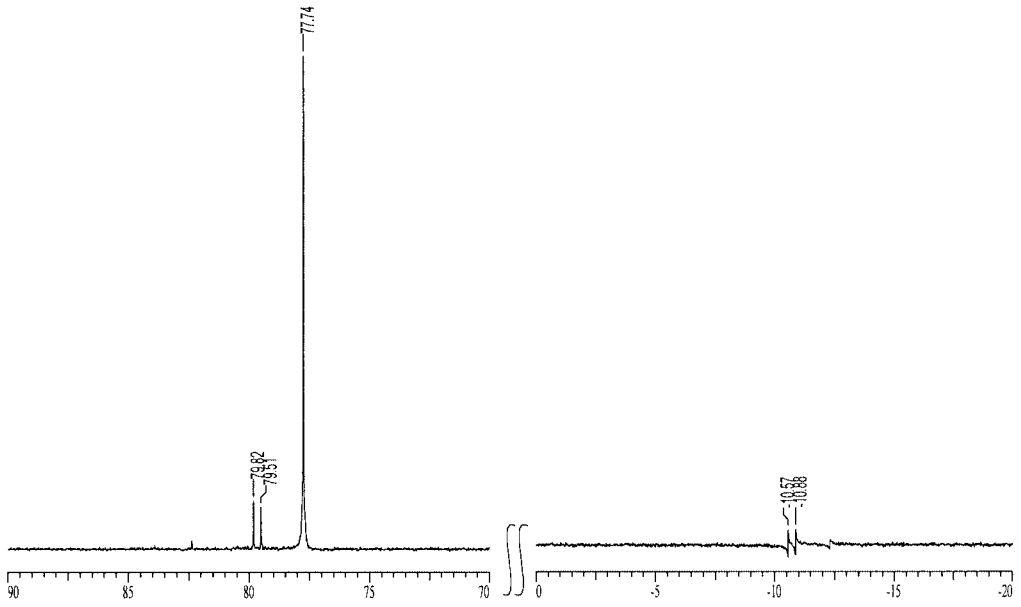

Figure 1. ^{31}P NMR spectrum of the crude product from the synthesis of $[KCpFe(CN)_2]_2$-μ-dppe (**4**) with baseline omitted from 0 to 70 ppm

corresponding diphosphane in a 1:1 mixture of acetonitrile/methanol. A small impurity of the singly bonded phosphorus derivative, such as $KCpFe(CN)_2$dppe, often accompanies these syntheses. Figure 1 depicts the ^{31}P NMR spectrum of the crude product resulting from the reaction of $KCpFe(CN)_2(CO)$ with 0.5 equiv. of dppe, where in addition to the desired product **4** ($\delta^{31}_P = 78.2$ ppm) two weak ^{31}P signals at $\delta = 79.7$ and -10.8 ppm with ^{31}P coupling constants of 38.3 Hz are observed corresponding to bound and free phosphane, respectively. Varying the number of $-CH_2-$ units linking the phosphorus donors from 2 to 4 allows for control of the orientation of the cyanide ligands with respect to one another (vide infra). As anticipated, the ν(CN) vibrational modes in complexes **4**, **5**, and **6** are virtually identical (see Table 1) since all of the bridging phosphane ligands are of similar basicity.

A more contrasting example of a bridging phosphane can be seen in the bis(diphenylphosphanyl)acetylene case, complex **7**. This short-chain bridging phosphane is comprised of a linear alkylene backbone, with diminished electron-donating ability compared to its dppe counterpart, **4**. The decrease in basicity is readily apparent in the ν(CN) values in complex **7** which are on average 10 cm^{-1} higher than those of complex **4**. Furthermore, the linear nature of the phosphane prohibits the cyanide ligands of the bis(iron) complex from interacting at the same metal center. One might imagine this bis(cyanometalate) behaving as a strut which links metal centers to form chain-like structures.

The solid-state structures of representative examples of these phosphane-substituted (cyclopentadienyl)iron dicyanide salts have been examined by X-ray crystallography. Single crystals of compounds **1** and **4** were grown from a concentrated methanol solution by slow concentration over several weeks at ambient temperature. Compound **6** was crystallized from THF/hexane at 10 °C, whereas single crystals of **3** were obtained by slow concentration of a hexane solution at room temperature. Selected bond lengths and angles of compounds **1**, **3**, **4**, and **6** are listed in Table 2.

Table 2. Selected bond lengths [Å] and angles [°] for compounds **1**, **3**, **4**, and **6**

	1	**3**	**4**	**6**
Fe(1)−C(6A)	1.880(8)	1.889(3)	1.871(12)	1.847(9)
Fe(1)−P(1)	2.175(2)	2.2025(8)	2.180(3)	2.183(2)
C(6A)−N(1A)	1.166(8)	1.156(3)	1.178(13)	1.163(10)
N(1A)−K(1)	2.847(5)	–	2.980(9)	2.982(8)
N(2A)−K(1)	–	–	3.086(10)	3.138(7)
N(2B)−K(2)	–	–	2.971(9)	–
N(1B)−K(1)	–	–	2.828(9)	–
N(2B)−K(1)	–	–	–	2.781(9)
N(1B)−K(2)	–	–	2.999(9)	2.744(7)
C(6A)−Fe(1)−C(7A)	89.3(3)	–	91.7(5)	91.6(3)
C(6A)−Fe(1)−P(1)	93.9(2)	87.73(8)	89.7(3)	88.8(3)
C(6A)−N(1A)−K(1)	136.8(4)	–	87.5(7)	85.9(6)
P(1)−Fe(1)−P(2)	–	98.42(3)	–	–

The effect of replacing the carbonyl group with a phosphane donor can be seen in the metric data for the iron cyanide unit. Specifically, the iron−carbon(cyanide) distances in compounds **1**, **4**, and **6** are shorter than those seen in $KCpFe(CN)_2CO$, where an average Fe−CN distance of 1.911(8) Å was observed.[13,14] This subtle yet statistically relevant bond-length change is the result of replacing the good π-acceptor, CO, with a good donor ligand, phosphane. Concomitantly, the increase in bond order to the Fe−CN bond causes a decrease in the C−N triple-bond

character, where the C(6A)−N(1A) bond lengths in compounds **1**, **4**, and **6** are all longer than that determined in the CO analog [1.143(10) Å]. Although this is compelling crystallographic evidence, the decrease in the cyanide triple-bond order is more evident by observing the ν(CN) vibrational modes shift to lower frequencies as previously noted. As expected, the Fe−P bond lengths in compounds **1**, **4**, and **6** are quite similar, spanning the narrow range from 2.175(2) in **1** to 2.183(2) Å in **6**. In the diphosphane neutral derivative, **3**, there is a slight lengthening of the Fe−P bond where a distance of 2.2025(8) Å is observed. Although it is tempting to attribute the bond lengthening to an electronic effect, it might also be due to enhanced steric congestion about the iron center. Support for this latter explanation comes from the metric parameters obtained for the chelated CpFe(CN)(dppe) derivative. CpFe(CN)(dppe) was prepared by the method of Vahrenkamp and co-workers[5] and its solid-state structure defined by X-ray crystallography.[15] The average Fe−P bond length in this instance was found to be 2.1788(14) Å, which is indistinguishable from those seen in the anionic compounds **1**, **4**, and **6**. The thermal ellipsoid representations of these closely related neutral iron monocyanide derivatives, **3** and CpFe(CN)(dppe), are provided in Figure 2 and Figure 3. These drawings clearly illustrate the difference observed in the solid state of the orientation of the phenyl substituents of the phosphane ligands in **3** as compared with their imposed, sterically less demanding orientation seen in CpFe(CN)(dppe).

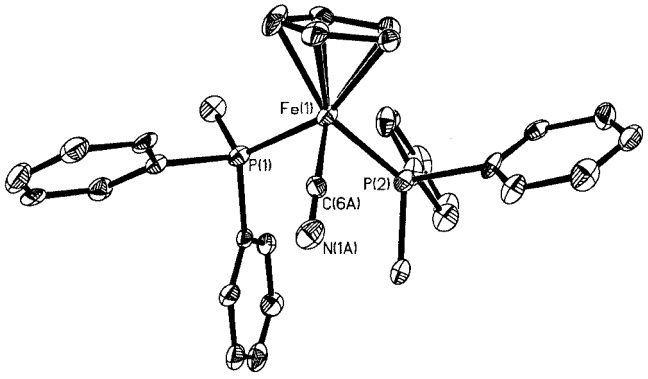

Figure 2. Thermal ellipsoid representation of CpFe(CN)-$(PPh_2Me)_2$ (**3**)

As noted in the thermal ellipsoid drawings in Figure 4, Figure 5 and Figure 6 of the salts, **1**, **4**, and **6**, in all instances the compounds pack in the crystal lattice so as to orient in such a manner as to maximize the number of cyanide−potassium interactions. These −CN−K interactions are either bridging or terminal in nature, with the two not being mutually exclusive. An instance of terminal interaction can be seen in Figure 4 between N(1A) and K(1), with an average distance of 2.847 Å. Potassium ions that bridge cyanide ligands on the same iron center, such as K(1) seen in Figure 5, display a stronger interaction with one of the cyanide nitrogen atoms. This is evidenced by a 0.1 Å

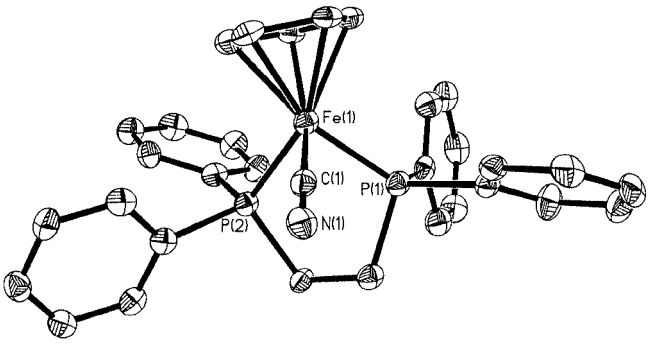

Figure 3. Thermal ellipsoid drawing of CpFe(CN)(dppe); selected bond lengths [A] and angles [°]: Fe(1)−P(2) 2.1747(14), Fe(1)−P(1) 2.1828(15), Fe(1)−C(1) 1.898(5), N(1)−C(1) 1.154(6); P(2)−Fe(1)−P(1) 84.76(6), C(1)−Fe(1)−P(2) 89.02(14), C(1)−Fe(1)−P(1) 88.43(14)

shorter interaction distance between N(1A) and K(1) as compared to that of N(2A)−K(1). In order to utilize these latter anionic metallocyanides as ligands towards other metal centers, the bridging diphosphane ligand must be flexible. That is, the orientation of the iron centers with respect to one another is controlled by the length of the chain between the Ph_2P- units. As is readily seen in Figure 5 of compound **4** the dppe bridge between the iron centers (n = 2) is sufficiently short so as to render it impossible for the four cyanide ligands on the two iron centers to become coplanar. The coplanarity of these four cyanide ligands is a requirement for providing mixed-metal diamond-shaped structures (vide infra). Upon lengthening the chain from n = 2 to n = 3 (**5**) or 4 (**6**) allows greater flexibility in the phosphane bridge, thereby, permitting the cyanide ligands to become coplanar in their chelation towards other metal centers (vide infra).

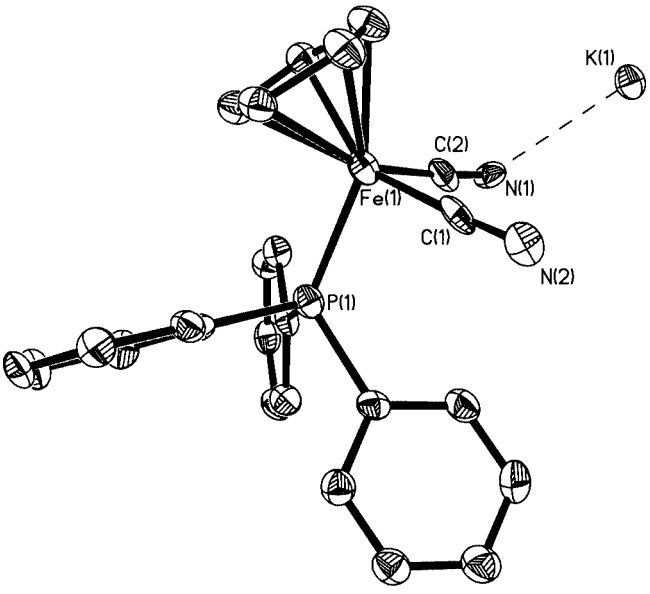

Figure 4. Thermal ellipsoid drawing of $KCpFe(CN)_2(PPh_3)$ (**1**) with solvent molecules and hydrogen atoms removed for clarity

Presently, we report studies involving the use of the $CpFe(CN)_2$ units with bound phosphanes as anionic li-

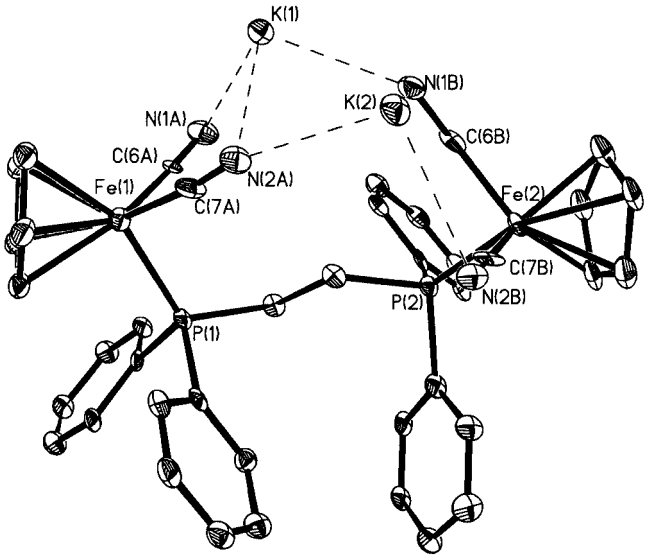

Figure 5. Thermal ellipsoid drawing of $[KCpFe(CN)_2]_2$-μ-dppe (**4**) with solvent molecules and hydrogen atoms removed for clarity

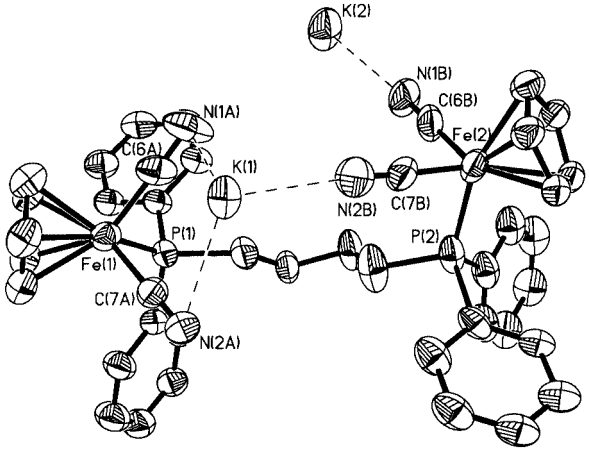

Figure 6. Thermal ellipsoid drawing of $[KCpFe(CN)_2]_2$-μ-dppb (**6**) with solvent molecules and hydrogen atoms removed for clarity

gands for the formation of double-metal cyanides. Specifically, the reaction of $KCpFe(CN)_2PPh_3$ with $Cu(CH_3CN)_4(BF_4)$ was carried out in acetonitrile to yield a fine yellow powder. This material was insoluble in all common organic solvents, which is in sharp contrast to its carbonylated analog.[16] In an effort to provide a soluble complex, a similar reaction was performed where an equivalent of PCy_3 was added to the copper(I) reagent prior to its addition to the iron dicyanide salt. This procedure led to the formation of a soluble double-metal cyanide derivative, complex **9**. Following the removal of acetonitrile, complex **9** was separated from the by-product KBF_4 salt by dissolution in dichloromethane. As anticipated for bridging cyanide ligands, the ν(CN) vibrational modes in complex **9** were shifted to higher frequencies compared to the corresponding values in the parent salt (see Table 1 and Table 3). Single crystals of **9** suitable for X-ray diffraction were grown by vapor diffusion of a CH_2Cl_2/hexane solution at 10 °C over a period of one week. A thermal-ellipsoid drawing of complex **9** is depicted in Figure 7, whereas selected bond lengths and angles are provided in Table 4.

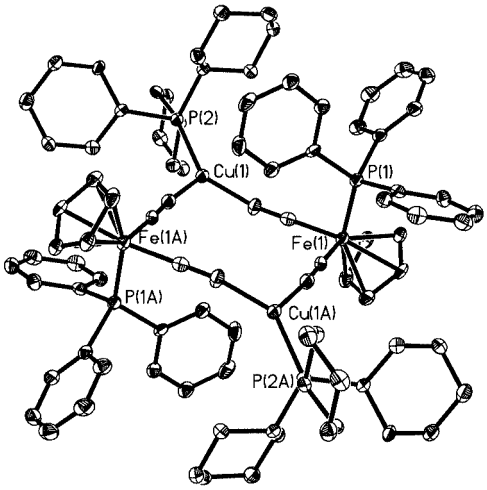

Figure 7. Thermal ellipsoid representation of $[CpFe(PPh_3)(\mu\text{-}CN)_2CuPCy_3]_2$ (**9**) with hydrogen atoms removed for clarity

The solid-state structure of complex **9** is similar to that seen for its $CpFe(CN)_2CO^-$-derived analog, $[\eta^5\text{-}C_5H_5Fe(CO)(\mu\text{-}CN)_2CuPCy_3]_2$.[16] That is, complex **9** exhibits a diamond-shaped motif composed of two $CpFe(PPh_3)$ fragments, two copper(I) centers, and four bridging CN^- ligands. The copper(I) centers display trigonal geometry as defined by the phosphorus and nitrogen donor groups. The iron-bound phosphane ligands lie on opposite sides of the metallacycle plane of the four metal atoms. The inversion center present in the structure of **9** demonstrates the metallacycle's high symmetry. Figure 8 illustrates the channels formed by the packing of complex **9** in the solid state, which

Table 3. Infrared [ν(CN)] and ^{31}P NMR spectral data for complexes **8**−**12**

Complex	Solvent	ν(CN) [cm^{-1}]	δ [ppm]
$[CpFe(PPh_3)(\mu\text{-}CN)_2Cu(CH_3CN)_2]_2$ [a] (**8**)	pyridine	2081, 2070	–
$[CpFe(PPh_3)(\mu\text{-}CN)_2Cu(PCy_3)]_2$ (**9**)	CH_2Cl_2	2085, 2078	84.7, 11.5
$[CpFe(\mu\text{-}CN)_2Cu(CH_3CN)_2]_2$-μ-dppp[a] (**10**)	pyridine	2075, 2065	–
$Cu(PCy_3)[CpFe(\mu\text{-}CN)_2]_2Cu(PCy_3)_2$-μ-dppp (**11**)	CH_2Cl_2	2089, 2083, 2077	74.2, 14.1, 11.2
$Cu(PCy_3)[CpFe(\mu\text{-}CN)_2]_2Cu(PCy_3)_2$-μ-dppb (**12**)	CH_2Cl_2	2082, 2077	74.3, 13.5, 10.7

[a] Complexes were only soluble in pyridine under which conditions the acetonitrile ligands on copper(I) are most likely displaced by pyridine.

Table 4. Selected bond lengths [Å] and bond angles [°] in complexes **9** and **11**

Complex **9**			
Fe(1)−C(1)	1.868(7)	Cu(1)−N(2)	1.949(7)
Fe(1)−C(2)	1.865(8)	Cu(1)−P(2)	2.1865(19)
Fe(1)−P(1)	2.173(2)	C(1)−N(1)	1.169(8)
Cu(1)−N(1)	1.917(6)	C(2)−N(2A)	1.168(8)
C(1)−Fe(1)−P(1)	92.4(2)	C(1)−N(1)−Cu(1)	153.6(6)
C(2)−Fe(1)−P(1)	87.0(2)	C(2)−N(2A)−Cu(1A)	171.8(6)
N(1)−C(1)−Fe(1)	178.6(6)	N(1A)−Cu(1A)−N(2A)	109.2(3)
N(2A)−C(2)−Fe(1)	178.0(6)	P(2)−Cu(1)−N(1)	133.0(2)
Complex **11**			
Fe(1)−C(1)	1.96(2)	Cu(1)−P(3)	2.324(7)
Fe(1)−C(2)	1.87(2)	Cu(1)−P(4)	2.287(7)
Fe(2)−C(3)	1.92(2)	Cu(2)−P(5)	2.206(8)
Fe(2)−C(4)	2.03(2)	C(1)−N(1)	1.18(2)
Fe(1)−P(1)	2.174(6)	C(2)−N(2)	1.19(2)
Fe(2)−P(2)	2.177(7)	C(3)−N(3)	1.13(2)
Cu(1)−N(1)	1.986(18)	C(4)−N(4)	1.07(2)
Cu(1)−N(3)	2.062(19)		
Cu(2)−N(2)	1.949(18)		
Cu(2)−N(4)	1.901(17)		
C(1)−Fe(1)−P(1)	90.9(6)	C(3)−N(3)−Cu(1)	175.0(19)
N(1)−C(1)−Fe(1)	178(2)	C(4)−N(4)−Cu(2)	164(2)
N(2)−C(2)−Fe(1)	173.9(18)	N(1)−Cu(1)−N(3)	100.4(7)
N(3)−C(3)−Fe(2)	177(2)	N(2)−Cu(2)−N(4)	105.0(8)
N(4)−C(4)−Fe(2)	177(2)	N(2)−Cu(2)−P(5)	123.3(5)
C(1)−N(1)−Cu(1)	159.3(18)	N(1)−Cu(1)−P(3)	100.8(5)
C(2)−N(2)−Cu(2)	163.9(16)	P(3)−Cu(1)−P(4)	127.3(3)

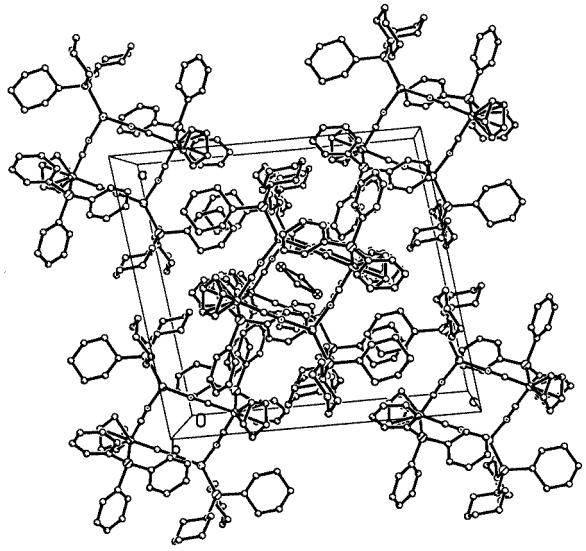

Figure 8. Crystal packing diagram of $[CpFe(PPh_3)(\mu\text{-}CN)_2CuPCy_3]_2$ (**9**), where the dichloromethane molecule is disordered

results in the inclusion of dichloromethane solvent molecules.

Utilization of two anionic $CpFe(CN)_2$ units bridged by diphosphanes containing three or four methylene linkers should afford particularly stable metallacycle derivatives with a second metal center as a result of the chelate effect. In a similar manner to the procedure employed in the synthesis of complex **9**, the iron cyanide salts (complexes **5** and **6**) were treated with $Cu(CH_3CN)_4(BF_4)$ in the presence of 2 equiv. of Cy_3P. The resulting mixed-metal cyanides **11** (dppp) and **12** (dppb) are soluble in dichloromethane, and as expected for bridging CN ligands, exhibit ν(CN) vibrational modes shifted to higher frequencies compared to the parent salts (see Table 1 and Table 3). The ^{31}P NMR spectra of both **11** and **12** display two broadened PCy_3 peaks indicative of two different phosphorus environments, with a single sharp signal for the iron-bound phosphorus atoms. The broadened phosphorus resonances for the PCy_3 ligands bound to Cu^I result from quadrupolar broadening i.e., for ^{63}Cu and ^{65}Cu, $I = 3/2$. Hence, spectroscopic data (IR and ^{13}P NMR) suggest the derivatives have similar structures.

Single crystals of **11** were grown by slow concentration of a concentrated hexanes solution of **11** over several days at ambient temperature, and were subjected to X-ray diffraction analysis. A thermal ellipsoid representation of complex **11** is shown in Figure 9, with selected bond lengths and angles given in Table 4. The crystal structure of **11** shows the familiar diamond-shaped motif with the bound phosphanes bridging the iron(II) centers. This phosphane-bridged form of the mixed-metal dimer forces both iron-bound phosphane ligands to be positioned on the same face

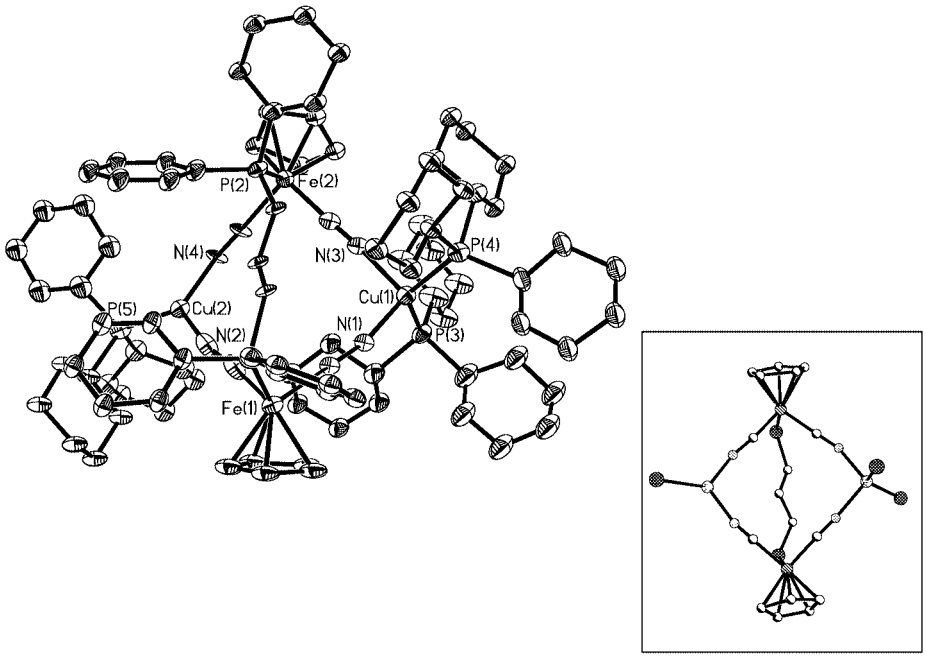

Figure 9. Thermal ellipsoid representation (drawn with 30% probability) of $Cu(PCy_3)[CpFe(\mu\text{-}CN)_2]_2Cu(PCy_3)_2$-μ-dppp (**11**); insert illustrates a ball-and-stick drawing of **11** where the substituents on the phosphane ligands are removed for clarity

of the metallacycle, with the two Fe−P distances being statistically equivalent at 2.174(6) and 2.177(7) Å. Interestingly, the basket shaped complex **11** crystallized with two PCy_3 ligands bonded to one Cu^I center, and one PCy_3 ligand attached to the other Cu^I center. This results in tetrahedral and trigonal-planar coordination geometries for the two copper centers, respectively. In addition to the differences in coordination geometries, the CN−Cu distances are shorter for Cu(2) as compared with Cu(1), i.e., the average CN−Cu(2) distance is 1.925(17) Å vs. the average CN−Cu(1) distance of 2.024(18) Å. This can be explained based on the higher Lewis acidity of Cu(2) resulting from fewer electron-donating PCy_3 ligands occupying its coordination sphere. The same effect is noted in the shorter Cu(2)−P(5) bond of 2.206(8) Å, as compared to the average Cu(1)−P bond length of 2.306(7)Å.

Unlike the $[Fe_2(CN)_4Cu_2]$ derivative containing a monodentate phosphane ligand bound to iron(II), as in complex **9**, complex **11** possesses *no* void channels for encompassing solvent molecules. This is best illustrated in their respective space-filling models depicted in Figure 10.

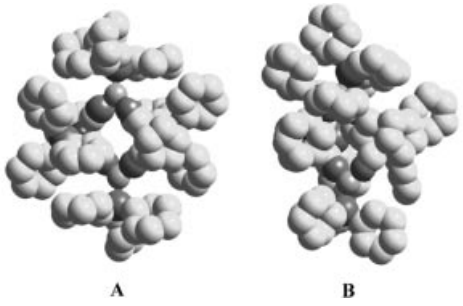

Figure 10. Space-filling model of: (A) $[CpFe(PPh_3)(\mu\text{-}CN)_2Cu(PCy_3)]_2$ (**9**) and (B) $Cu(PCy_3)[CpFe(\mu\text{-}CN)_2]_2Cu(PCy_3)_2$-μ-dppp (**11**)

Concluding Remarks

In summary, we have reported the syntheses and structures of several phosphane-substituted $CpFe(CN)_2$ salts obtained by photochemical decarbonylation of $KCpFe(CN)_2CO$ in methanol. The anions of these salts, which offer the opportunity for variation in steric and electronic modifications, were shown to serve as uninegative bridging ligands towards copper(I) centers. Unique among these derivatives was the preparation and characterization of the diphosphane-bridged iron species, $CpFe(CN)_2PPh_2-(CH_2)_n-PPh_2Fe(CN)_2Cp^{2-}$ ($n = 2-4$). These latter anions were shown to act as pincers to encapsulate (phosphane)copper(I) complexes, thereby leading to very stable diamond-shaped, two-dimensional $[Fe_2(CN)_4Cu_2]$, mixed-metal derivatives. These bridged (phosphane)metal anions may also serve to bind a variety of $M^{II}X^+$ or $M^{III}X_2^+$ ions in an analogous manner.[17]

Experimental Section

Methods and Materials: All manipulations were carried out using standard Schlenk techniques under argon unless otherwise stated. THF and hexane were dried by refluxing in the presence of sodium/benzophenone and distillation prior to use. Methanol was dried by distillation from magnesium turnings and iodine. Acetonitrile was dried by successive distillation from CaH_2 and P_2O_5. 1-Propanol was dried with molecular sieves and degassed by argon purge prior to use. All phosphanes were purchased from Strem Chemicals, ex-

cept for triphenylphosphane, which was purchased from Aldrich. Copper(I) oxide and nitrosyl tetrafluoroborate were obtained from Aldrich and Lancaster, respectively. $KCpFe(CN)_2(CO)$ was prepared by applying published procedures.[13,18] Unless otherwise stated, all photolysis reactions were performed using a mercury-arc 450-W UV immersion lamp purchased from Hanovia. The 200-mL water-cooled photolysis vessel was purchased from Ace Glass. CpFe(dppe)CN was synthesized according to the procedure described by Vahrenkamp and co-workers.[5] Copper tetrafluoroborate was prepared as described previously.[19]

Physical Measurements: All vibrational studies were carried out with a Mattson 6021 FTIR spectrometer, using a 0.1-mm CaF_2 sealed cell. ^1H and ^{31}P NMR were recorded with a 300-MHz Varian Unity Plus spectrometer (121.4 MHz, ^{31}P), with methanol as the solvent unless otherwise stated. Deuterated water was used as the lock solvent, and all spectra were referenced to an 85% phosphoric acid solution.

Synthesis of $KCpFe(CN)_2(PPh_3)$ (1): 100 mL of a 1:1 mixture of acetonitrile/methanol was added to $KCpFe(CN)_2(CO)$ (4.2 mmol, 1.0 g) and PPh_3 (4.2 mmol, 1.1 g) in a photolysis vessel. An argon purge was bubbled through the reaction slurry and the mixture was photolyzed for 2 h while monitoring the infrared spectra in the ν(CN) region at 30-min intervals to ensure complete replacement of CO. The crude orange product precipitated from the solution and the solvent was removed under vacuum. The isolated product was dissolved in 1-propanol and filtered through a frit containing Celite. The solvent was once again removed under vacuum, and the solid washed with pentane to give **1** in 88% yield (1.7 g). Single crystals of **1** were obtained by slow concentration of a methanol solution of **1** at room temperature over several days. $C_{25}H_{20}FeKN_2P{\cdot}CH_3CN$ (515.3): calcd. C 62.92, H 4.50, N 8.15; found C 62.54, H 4.67, N 8.03.

Synthesis of $KCpFe(CN)_2(PPh_2Me)$ (2): 100 mL of methanol was added to $KCpFe(CN)_2(CO)$ (1.0 mmol, 0.25 g) and PPh_2Me (1.0 mmol, 0.21 g) in a photolysis vessel and the solution was photolyzed with IR monitoring as described for the preparation of **1**. The reaction solution was concentrated to dryness under vacuum to yield an orange powder. The solid product was washed repeatedly with hexane and dried to provide **2** in a 70% yield (0.31 g). $C_{20}H_{18}FeKN_2P{\cdot}CH_3OH$ (444.3): calcd. C 56.77, H 4.99, N 6.30; found C 55.97, H 5.08, N 6.52.

Synthesis of $CpFe(CN)(PPh_2Me)_2$ (3): Photolysis of $KCpFe(CN)_2CO$ (1.8 mmol, 0.45 g) and PPh_2Me (7.4 mmol, 1.5 g) in 100 mL of methanol was carried out in a photolysis vessel under argon. Upon reaction completion, ca. 30 min as revealed by infrared spectroscopy in the ν(CO) region, the solution was concentrated to dryness under vacuum and the product was dissolved in hexane. The solution was filtered through a glass frit containing Celite to remove any remaining impurities and the product, complex **3**, was isolated upon removing the solvent under vacuum in a yield of 56% (0.52 g). Single crystals of **3** were grown by slow concentration of a hexane solution at ambient temperature. $C_{32}H_{31}FeNP$ (516.4): calcd. C 70.21, H 5.71; found C 69.92, H 5.86.

Synthesis of $[KCpFe(CN)_2]_2$-μ-$[Ph_2P-(CH_2)_n-PPh_2]$ [n = 2 (4), n = 3 (5), n = 4 (6), C≡C instead $(CH_2)_n$ (7)]: These four derivatives were prepared in a similar manner by photolysis of $KCpFe(CN)_2CO$ and the diphosphanes in a 1:1 mixture of acetonitrile/methanol over a 60-min reaction period in a photolysis vessel. After the photolysis, the reaction solution was concentrated to dryness under vacuum to produce an orange solid product. The crude product was dissolved in 1-propanol and filtered through a frit containing Celite. Subsequent to removal of solvent, the product was washed repeatedly with hexane and dried under vacuum. Specifics of reactions: $KCpFe(CN)_2CO$ (4.2 mmol, 1.0 g) and dppe (1.0 mmol, 0.40 g) provided **4** in an 85% yield (0.70 g). X-ray quality crystals were grown by slow concentration of a solution of **4** in methanol at ambient temperature over several weeks. $C_{40}H_{34}Fe_2K_2N_4P_2{\cdot}6CH_3OH$ (1014.5): calcd. C 54.44, H 5.76; found C 55.01, H 5.52. $KCpFe(CN)_2CO$ (4.6 mmol, 1.1 g) and dppp (1.6 mmol, 0.64 g) provided **5** in an 81% yield (1.08 g). Single crystals of **5** were grown as described for compound **4**. $C_{41}H_{36}Fe_2K_2N_4P_2{\cdot}6CH_3OH$ (1028.5): calcd. C 54.87, H 5.88, N 5.45; found C 55.10, H 5.55, N 5.70. $KCpFe(CN)_2(CO)$ (1.6 mmol, 0.40 g) and dppb (0.70 mmol, 0.30 g)provided **6** in a 61% yield (0.36 g). Single crystals of **6** were grown by vapor diffusion of hexane into a THF solution of **6** maintained at 10° for approximately one week. $C_{42}H_{38}Fe_2K_2N_4P_2{\cdot}2THF{\cdot}2H_2O{\cdot}CH_3OH$ (1062.6): calcd. C 58.51, H 5.97; found C 58.97, H 5.62. $KCpFe(CN)_2CO$ (3.1 mmol, 0.75 g) and dppa (1.0 mmol, 0.41 g) provided **7** in an 82% yield (0.67 g).

Synthesis of $[CpFe(PPh_3)(\mu\text{-}CN)_2Cu(CH_3CN)_2]_2$ (8): A solution of $Cu(CH_3CN)_4(BF_4)$ (0.08 g, 0.25 mmol) in 15 mL of CH_3CN was transferred via cannula to a Schlenk flask containing $KCpFe(CN)_2PPh_3$ (0.12 g, 0.25 mmol) in 10 mL of CH_3CN. The reaction mixture was stirred at ambient temperature for 1 h to afford a yellow precipitate. Upon removal of the solvent under vacuum a fine yellow powder was isolated. Among common organic solvents, only pyridine was found to solubilize the yellow solid product.

Synthesis of $[CpFe(PPh_3)(\mu\text{-}CN)_2Cu(PCy_3)]_2$ (9): $Cu(CH_3CN)_4(BF_4)$ (0.06 g, 0.19 mmol) in 15 mL of CH_3CN was transferred via cannula to a Schlenk flask containing 0.054 g (0.19 mmol) of PCy_3 in 10 mL of CH_3CN, and the solution was stirred at ambient temperature for 1 h prior to adding 0.091 g (0.19 mmol) of $KCpFe(CN)_2PPh_3$ in CH_3CN. The reaction mixture was stirred for an additional hour during which time a turbid yellow solution was observed. The solvent was removed under vacuum and the product was redissolved in dichloromethane, leaving behind a white precipitate of KBF_4 which was removed by filtration through a frit containing Celite. Evaporation of the solvent from the filtrate yielded a fine yellow powder in a yield of 62% (0.092 g). Single crystals of **9** were grown by vapor diffusion of CH_2Cl_2/hexane at 10 °C over a period of one week. $C_{86}H_{106}Cu_2Fe_2N_4P_4{\cdot}CH_2Cl_2$ (1651.1): calcd. C 63.58, H 6.62, N 3.41; found C 62.98, H 6.54, N 3.29.

Synthesis of $[CpFe(\mu\text{-}CN)_2Cu(CH_3CN)_2]_2$-μ-dppp (10): A solution of 0.1 g (0.32 mmol) of $Cu(CH_3CN)_4(BF_4)$ in 15 mL of CH_3CN was transferred via a cannula to a flask containing 0.133 g (0.16 mmol) of $[KCpFe(CN)_2]_2$-μ-dppp in 10 mL of CH_3CN. The solution was stirred at room temperature for 1.5 h to yield a yellow precipitate. The solvent was evaporated under vacuum to give a fine yellow powder. Among common organic solvents, only pyridine was found to solubilize the precipitate.

Synthesis of $Cu(PCy_3)[CpFe(\mu\text{-}CN)_2]_2Cu(PCy_3)_2$-μ-dppp (11): $Cu(CH_3CN)_4(BF_4)$ (0.03 g, 0.1 mmol) in acetonitrile (15 mL) was added via cannula to a Schlenk flask containing PCy_3 (0.054 g, 0.2 mmol). The solution was stirred at room temperature for 1 h. The mixture was transferred via cannula to a second flask containing $[KCpFe(CN)_2]_2$-μ-dppp (0.04 g, 0.05 mmol) in CH_3CN (10 mL), and the reaction mixture was stirred at room temperature for 1.5 h to afford a turbid yellow solution. The solvent was removed under vacuum and the product dissolved in dichlorometh-

Table 5. X-ray crystallographic data for $KCpFe(CN)_2(PPh_3)$ (**1**), $CpFe(PPh_2Me)_2(CN)$ (**3**), $[KCpFe(CN)_2]_2\mu$-dppe (**4**), $[KCpFe(CN)_2]_2\mu$-dppb (**6**), $[CpFe(PPh_3)(\mu\text{-}CN)_2Cu(PCy_3)]_2$ (**9**), and $Cu(PCy_3)[CpFe(\mu\text{-}CN)_2]_2Cu(PCy_3)_2$-μ-dppp (**11**)

	1	**3**	**4**	**6**	**9**	**11**
Empirical formula	$C_{25}H_{20}FeKN_2P\cdot CH_3CN$	$C_{32}H_{31}FeNP_2\cdot H_2O$	$C_{40}H_{34}Fe_2K_2N_4P_2\cdot 6CH_3OH$	$C_{42}H_{38}Fe_2K_2N_4P_2\cdot 2THF\cdot 2H_2O\cdot CH_3OH$	$C_{86}H_{106}Cu_2Fe_2N_4P_4\cdot CH_2Cl_2$	$C_{105}H_{159}Cu_2Fe_2N_4P_5$
Formula mass [g/mol]	515.40	563.37	1002.71	1061.88	1643.4	1870.99
Crystal system	triclinic	monoclinic	triclinic	monoclinic	monoclinic	triclinic
Space group	$P\bar{1}$	$P2_1/c$	$P\bar{1}$	$P2_1/c$	$P2_1/n$	$P\bar{1}$
Z·	2	4	2	4	4	2
a [Å]	7.962(2)	9.959(2)	12.302(3)	14.4418(9)	17.248(3)	12.925(13)
b [Å]	9.180(2)	14.458(3)	13.550(3)	34.147(2)	12.686(2)	17.871(18)
c [Å]	17.425(4)	19.892(4)	16.119(3)	10.2584(6)	18.556(4)	23.75(2)
α [°]	92.230(4)	90	92.873(4)	90	90	98.23(2)
β [°]	97.864(4)	102.344(4)	94.038(4)	94.7500(10)	96.929(4)	101.62(2)
γ [°]	113.721(4)	90	115.227(4)	90	90	104.79(2)
Volume [Å^3]	1148.8(5)	2798.0(10)	2415.0(9)	5041.5(5)	4030.7(14)	5086(9)
$d_{calcd.}$ [g/cm^3]	1.490	1.337	1.379	1.399	1.354	1.222
Temperature [K]	110(2)	110(2)	110(2)	110(2)	110(2)	110(2)
Wavelength [Å]	0.71073	0.71073	0.71073	0.71073	0.71073	0.71073
Abs. coeff. [mm^{-1}]	0.929	0.679	–	0.854	1.066	0.817
Goodness of fit on F^2	0.867	0.801	0.757	0.899	0.599	0.662
R[a] (%)	6.28	4.59	8.60	7.18	6.69	10.37
(%)						
R_w[b] (%)	16.46	10.01	19.25	18.47	18.66	50.41

[a] $R = \Sigma|F_o| - |F_c|/\Sigma|F_o|$. [b] $Rw = \{[\Sigma w(F_o^2 - F_c^2)^2]/[\Sigma w(F_o^2)^2]\}^{1/2}$.

ane. The salt by-product was removed by filtration through Celite, and the solvent evaporated to give a yellow powder of **11** in a yield of 54% (0.050 g). Crystals suitable for X-ray diffraction studies were obtained from hexanes by slow concentration at ambient temperature over several days. $C_{105}H_{159}Cu_2Fe_2N_4P_5$ (1871.2): calcd. C 67.40, H 8.57, N 2.99; found C 66.92, H 8.43, N 3.05.

Synthesis of $Cu(PCy_3)[CpFe(\mu\text{-}CN)_2]_2Cu(PCy_3)_2$-μ-dppb (12): $Cu(CH_3CN)_4(BF_4)$ (0.022 g, 0.07 mmol) in 15 mL of CH_3CN was transferred via cannula to a Schlenk flask containing PCy_3 (0.04 g, 0.14 mmol) in 10 mL of CH_3CN. The reaction mixture was stirred at room temperature for 1 h and transferred to a second flask containing 0.03 g (0.035 mmol) of $[KCpFe(CN)_2]_2$-μ-dppb in 10 mL of CH_3CN. The solution was stirred for 1.5 h to give a turbid yellow solution. Upon removal of the CH_3CN solvent under vacuum, the product was redissolved in dichloromethane and filtered through Celite to remove KBF_4. A yellow product of **12** was obtained in a yield of 39% (0.026 g) following the evaporation of solvent and was recrystallized from hexanes by slow concentration at ambient temperature. $C_{106}H_{161}Cu_2Fe_2N_4P_5$ (1885.2): calcd. C 67.54, H 8.61; found C 68.05, H 8.48.

X-ray Crystallography: Orange single crystals of compounds **1**, **3**, **4**, **6**, and CpFe(CN)(dppe), and yellow crystals of **9** and **11** were coated with paratone and mounted on a glass fiber using apiezon grease at ambient temperature. The crystals were placed on a Bruker SMART 1000 diffractometer equipped with a CCD detector. The crystals were placed in a nitrogen cold stream maintained at 110 K. More than a hemisphere of data was collected on each crystal over three batches of exposures using Mo-K_α radiation (λ = 0.71073 Å). A fourth set of data was measured and compared to the initial set to monitor and correct for decay, which was negligible in all cases. Details of crystal data for all compounds examined are found in Table 5. Systematic absences and intensity statistics were used in space-group determination. All structures were solved by direct methods. Anisotropic structure refinements were achieved using full-matrix least-squares techniques on all non-hydrogen atoms. All hydrogen atoms were placed in idealized positions based on hybridization, with isotropic thermal parameters fixed at 1.2 or 1.5 times the value of the attached atom. All atom scattering factors were obtained from the *International Tables for X-ray Crystallography*, vol. C. For all compounds, data collection and cell refinement, SMART;[20] data reduction, SAINTPLUS (Bruker[21]); programs used to solve structures, SHELXS-86 (Sheldrick[22]); programs used to refine structures, SHELXL-97 (Sheldrick[23]); molecular graphics and to prepare material for publication, SHLXTL-Plus version 5.0 (Bruker[24]). CCDC-211280 (**1**), -211281 (**3**), -211282 (**4**), -211283 (**6**), -211284 (**9**), -211285 (**11**) and -213786 [CpFe(CN)dppe] contain the supplementary crystallographic data for this paper. These data can be obtained free of charge at www.ccdc.cam.ac.uk/conts/retrieving.html [or from the Cambridge Crystallographic Data Centre, 12 Union Road, Cambridge CB2 1EZ, UK; Fax: (internat.) + 44-1223/336-033; E-mail: deposit@ccdc.cam.ac.uk].

Acknowledgments

Financial support from the National Science Foundation (CHE 99-10342 and CHE 02-34860), and CHE 98-07975 for purchase of X-ray equipment, the Robert A. Welch Foundation, and by the Texas Advanced Research Technology Program (Grant No. 0390-1999) is greatly appreciated.

[1] K. R. Dunbar, R. A. Heitz, *Prog. Inorg. Chem.* **1997**, *45*, 283–391.
[2] A. M. Golub, H. Kohler, V. V. Skopenko (Eds.), *Chemistry of Pseudohalides*, Elsevier, New York, **1986**, pp. 142–160.
[3] K. K. Klausmeyer, T. B. Rauchfuss, S. R. Wilson, *Angew. Chem. Int. Ed.* **1998**, *37*, 1694–1696.
[4] D. L. Reger, *Inorg. Chem.* **1975**, *14*, 660–664.

[5] G. N. Richardson, U. Brand, H. Vahrenkamp, *Inorg. Chem.* **1999**, *38*, 3070−3079.
[6] G. N. Richardson, H. Vahrenkamp, *J. Organomet. Chem.* **2000**, *597*, 38−41.
[7] See: D. J. Darensbourg, J. C. Yarbrough, C. Ortiz, C. C. Fang, *J. Am. Chem. Soc.* **2003**, *125*, 7586−7591 and references cited therein.
[8] W. J. Kruper, Jr., D. J. Swart, U. S. Patent 4,500,704, **1985**.
[9] D. J. Darensbourg, W.-Z. Lee, M. J. Adams, J. C. Yarbrough, *Eur. J. Inorg. Chem.* **2001**, 2811−2822.
[10] C. A. Tolman, *Chem. Rev.* **1977**, *77*, 313−348.
[11] M. M. Rahman, H. Y. Liu, A. Prock, W. P. Giering, *Organometallics* **1987**, *6*, 650−658.
[12] T. L. Brown, *Inorg. Chem.* **1992**, *31*, 1286−1294.
[13] C.-H. Lai, W.-Z. Lee, M. L. Miller, J. H. Reibenspies, D. J. Darensbourg, M. Y. Darensbourg, *J. Am. Chem. Soc.* **1998**, *120*, 10103−10114.
[14] D. J. Darensbourg, J. H. Reibenspies, C.-H. Lai, W.-Z. Lee, M. Y. Darensbourg, *J. Am. Chem. Soc.* **1997**, *119*, 7903−7904.
[15] Crystal for CpFe(CN)(dppe)·CH_2Cl_2: $C_{33}H_{31}C_{12}FeNP_2$ (630.28), monoclinic, $P2_1/n$, a = 12.842(2), b = 8.8075(16), c = 25.732(5) Å, β = 90.824(4)°, V = 2910.2(9) Å^3, Z = 4, $\rho_{calcd.}$ = 1.439 Mg/m^3, Mo-K_α radiation, λ = 0.71073 Å, T = 293(2) K, 17540 measured reflections, 6613 unique, μ = 0.836 mm^{-1}, $R1$ [$I > 2\sigma(I)$] = 0.0623, $wR2$ = 0.1341, GOF = 0.882, no. of parameters = 352.
[16] D. J. Darensbourg, W.-Z. Lee, M. J. Adams, D. L. Larkins, J. H. Reibenspies, *Inorg. Chem.* **1999**, *38*, 1378−1379.
[17] D. J. Darensbourg, M. J. Adams, J. C. Yarbrough, *Inorg. Chem.* **2001**, *40*, 6543−6544.
[18] C. E. Coffey, *J. Inorg. Nucl. Chem.* **1963**, *25*, 179−185.
[19] G. J. Kubas, *Inorg. Synth.* **1979**, *19*, 90−92.
[20] *SMART 1000 CCD*, Bruker Analytical X-ray Systems, Madison, WI, USA, **1999**.
[21] *SAINT-Plus*, version 6.02, Bruker, Madison, WI, USA, **1999**.
[22] G. Sheldrick, *SHELXS-86, Program for Crystal Structure Solution*, Institut für Anorganische Chemie der Universität, Göttingen, Germany, **1986**.
[23] G. Sheldrick, *SHELXL-97, Program for Crystal Structure Refinement*, Institut für Anorganische Chemie der Universität, Göttingen, Germany, **1997**.
[24] *SHELXTL*, version 5.0, Bruker, Madison, WI, USA, **1999**.

Received May 21, 2003

